Lasers in Surgery and Medicine 20:179–187 (1997)

Modelling the Assessment of Port Wine Stain Parameters From Skin Surface Temperature Following a Diagnostic Laser Pulse

Shimon Gabay, PhD,[1,2] Gerald W. Lucassen, PhD,[1] Wim Verkruysse, MSc,[1] and Martin J.C. van Gemert, PhD[1]*

[1]Laser Centre, Academic Medical Centre, University of Amsterdam, The Netherlands
[2]Laser Group, NRCH, Beer-Sheva, Israel

Background and Objective: **Laser treatment of port wine stains (PWS) has become an established clinical modality over the past decade. However, in some cases full clearance of the PWS cannot be achieved. To improve the clinical results, it is necessary to match the laser treatment parameters to the PWS anatomy on an individual patient basis. Therefore, knowledge of the PWS structure is of great importance. The objective of this study is to describe a diagnostic method to assess the PWS blood vessels depth and diameter from the skin surface temperature-time course following a diagnostic laser pulse.**
Study Design/Materials and Methods: **The Monte Carlo (MC) method was used to calculate the deposited laser energy into a port wine stain skin model following irradiation by a diagnostic laser pulse at 577 nm. The heat equation was solved numerically, using the deposited energy profile as the source term, yielding the temperature-time course at the skin surface. Subtraction of "bloodless" skin signal from that of the skin containing blood vessels gives us the net contribution of a heated dermal blood vessel to the skin surface temperature-time behaviour.**
Results: **The net blood vessel signal shows heat-diffusion behaviour and was found to be sensitive to the dermal blood vessel depth and diameter. The time delay for the peak signal temperature to occur depends quadratically on the blood vessel depth. The peak temperature relates linearly to the blood vessel diameter. The degree of epidermal melanin content can also be determined from the immediate temperature rise of the signal.**
Conclusion: **The proposed method easily enables assessment of the blood vessel depth and diameter as well as the epidermal melanin content in a skin model. The method can be applied to a real PWS when using the adjacent normal skin as a reference.**
Lasers Surg. Med. 20:179–187, 1997. **© 1997 Wiley-Liss, Inc.**

Key words: bioheat equation; heat diffusion; laser treatment; modelling; monte carlo; port wine stains; thermocamera; vascular lesion

INTRODUCTION

Port wine stains (PWS) are pink to purple vascular skin lesions characterized by an enlarged number, or enlarged diameter [1,2], of dermal blood vessels. Laser treatment of PWS is based on selective heat deposition into the ectatic dermal blood vessels [3] to produce irreversible

Contract grant sponsor: Dutch Organization for Scientific Research (NWO).

*Correspondence to: Prof. Dr. Martin J.C. van Gemert, Laser Center, Academic Medical Center, University of Amsterdam, Meibergdreef 9, 1105 AZ Amsterdam ZO, The Netherlands.

Accepted for publication 19 January 1996.

thermal damage in these target vessels. Clearance of the PWS can be achieved while the surrounding connective tissue is kept intact [4,5]. The "best" laser wavelength, defined as the wavelength that produces the deepest vascular injury in the dermis, is predicted to depend on the vascular anatomy of the PWS [6]. In addition, the "best" pulse duration for selective photothermolysis of a blood vessel is predicted to depend on the diameter of that vessel [3]. As a consequence, methods are currently being developed that allow noninvasive assessment of PWS parameters, such as concentration and size of ectatic dermal blood vessels. One of such methods uses the heat produced in the blood vessels after absorbing the light energy, which diffuses to the skin surface and induces a rise in skin surface temperature. The time for diffusion to the surface depends on the depth of the blood vessels in the skin, deeper vessels producing longer delayed temperature signals. Therefore, skin surface temperature-time behaviour following irradiation by a diagnostic laser pulse contains information related to the depth of the blood vessels and other light absorbers. Pulse photothermal radiometry (PPTR) was used [7–9] to measure the skin surface temperature-time behaviour typically consisting of an immediate temperature increase, induced by the heat absorbed in the epidermis, followed by a second, delayed, peak or by a monotonic decreasing profile, depending on the amount of energy absorbed in the deeper skin layers. Algorithms are being developed [8,9] to deduce the depth of the different absorbing structures from the measured surface temperature-time course.

The techniques described above aim to deduce the PWS vascular parameters from the skin surface temperature-time behaviour induced by different skin layers where only 1–10% [1] of the dermal volume is occupied by blood vessels and the rest is connective tissue. However, also the connective tissue absorbs some laser energy (absorption coefficient $\mu_{a,dermis} = 2.2\ cm^{-1}$ of the dermis is much less than that of blood $\mu_{a,blood} = 354\ cm^{-1}$ or epidermis $\mu_{a,epidermis} = 18\ cm^{-1}$ at wavelength 577 nm [10]) that contributes to the skin surface temperature signal. We hypothesize that a more precise deduction of PWS vascular parameters will result when the net contribution of the blood vessels to the skin surface temperature signal is known.

It is the purpose of this study to explore the feasibility of using a "bloodless" skin (e.g., the normal skin adjacent to the PWS lesion) to assess the contribution of all other chromophores to the skin surface temperature. Using this as a reference allows evaluation of the net contribution of the blood vessels to the skin temperature. We show that this signal can be used to deduce the blood vessel diameter and depth, as well as the degree of melanin content in the epidermis. The skin surface temperature response to a diagnostic laser pulse is modelled using a Monte Carlo program for evaluation of the spatial distribution of fluence rate and energy deposition, and a second-order finite difference numerical code for solving the heat equation using the deposited energy from the Monte Carlo program as a source term.

MATERIALS AND METHODS

Skin Model

The skin model used in this study is an extension of the model of van Gemert et al. [11] and is similar to that used by Smithies and Butler [12]. The skin model consists of two layers: the epidermis (60 μm thick) and dermis (940 μm thick) as shown in Figure 1. The melanin is assumed to be homogeneously distributed within the epidermis, and straight cylindrical blood vessels are embedded in the dermis. Each blood vessel is characterized by its diameter d and location $r(x,z)$. The number of blood vessels, as well as their diameter and location, can be varied (at present up to a maximum of 16 vessels, limited by allocation of memory of our PC) to simulate different PWS anatomies. A collimated laser beam of 2 mm spot size diameter, 450 μs pulse duration, $3 J/cm^2$ energy density, and 577 nm wavelength is incident in the z direction (at $x = 0$) normal to the epidermis, with the air-skin interface located at $z = 0$. The laser beam has a top hat spatial distribution. The optical parameters [10] of epidermis, dermis, and blood vessels are summarized in Table 1, where μ_a is the absorption coefficient in cm^{-1}, μ_s is the scattering coefficient in cm^{-1}, g is the mean cosine of the angular distribution of scattering, assuming a Henyey-Greenstein phase function [13], and n is the index of refraction. The 577 nm wavelength was theoretically preferred for blood vessel diagnosis, because of its high absorption by the oxyhaemoglobin resulting in a maximal signal when using a low energy diagnostic laser pulse.

Monte Carlo Program

The spatial distribution of light inside the skin, following laser irradiation, is calculated by

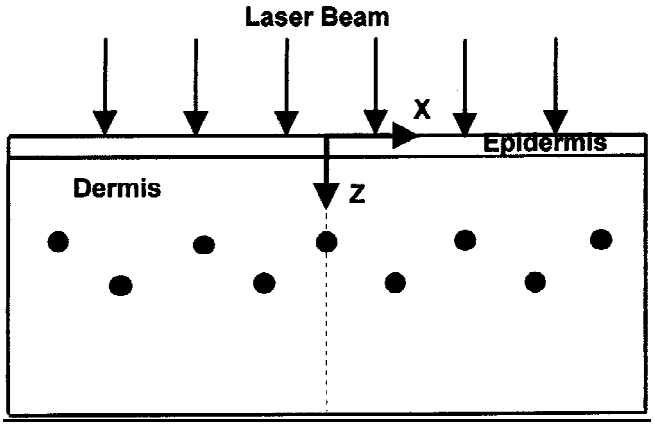

Fig. 1. Skin tissue model and laser irradiation behaviour. The melanin pigments are homogeneously distributed within the 60-μm-thick epidermis and the cylindrical blood vessels are embedded in the dermis. Each blood vessel is characterized by its diameter d and its location (*x,z*) of the center of the vessel.

TABLE 1. Optical Parameters of the Epidermis, Dermis, and Blood (oxyhaemoglobin), for 577 nm Wavelength*

	μ_a [cm^{-1}]	μ_s [cm^{-1}]	g	n
Epidermis	18.5	480	0.787	1.37
Dermis	2.2	210	0.787	1.37
Blood	354	468	0.995	1.33

*After Verkruysse et al. [10].

the Monte Carlo method (MC), which gives a statistically exact solution of light transport in a turbid medium [13]. The code is an extended version of that by Keijzer [14] written in Turbo Pascal and runs on PC. The details of this MC version are described elsewhere [15]. The optical parameters [10], the dimensions of the tissue layers, the location of the blood vessels, and the laser beam diameter are input data for the MC program. The tissue volume is divided into 20 × 20 × 20 μm^3 volume units oriented along the *x,y* and *z* axes. The photons are launched from a circular laser beam normal to the epidermis, where each photon has an initial weight W = 1. The "weighted method" is used where at each scatter event a fraction $\mu_a/(\mu_a + \mu_s)$ of the actual weight W is absorbed. These absorbed fractions (or deposited energy fractions) are scored in an array at each box in a x–z slice of 20 μm thickness. Each photon is followed until it reaches a weight less than the critical weight $W_{cr} = 0.0001$. This actually means that 10,000 photons are launched simultaneously, which improves the statistics in the result. The program output thus contains the deposited energy *D(r)[J/cm^3]* in any unit volume at coordinate *r.* Running the program for 10^6 photons was found to be adequate for obtaining reproducible results for runs with a single blood vessel, in case of multiple vessels (up to 16 vessels) 2×10^6 photons were used. A typical run of 2×10^6 photons for 16 blood vessels took ~ 10 hours on a IBM PC (486DX, 66 mhz). The total run time also depends on the chosen critical weight.

Heat Equation Program

The temperature profile *T(r,t)* follows from the heat diffusion equation:

$$\rho\, C \frac{\partial T(r,t)}{\partial t} = D(r)P(t) + \eta \nabla^2 T(r,t) \qquad (1)$$

with the density $\rho = 10^3$ kg/m^3, heat capacity C = 4.05×10^3 J/kg °C and heat conductivity η = 0.58 W/m°C of the skin, respectively. We use the heat equation instead of the bio-heat equation since we neglect the heat transfer from blood flow, because this effects much longer time scales (seconds to minutes) than that used here (millisecond). *T(r,t)* is the temperature rise at position *r=x,y,z* and at time *t. D(r)* is the deposited energy [J/m^3] at position *r,* which follows from the Monte Carlo simulation for the skin and blood vessel geometry chosen. The temporal profile *P(t)* is a normalized Gaussian, which to first-order approximation resembles a realistic dye laser pulse:

$$P(t) = \frac{1}{\sigma\sqrt{2\pi}} \exp((t - t_0)^2 / 2\sigma^2) \quad [s^{-1}] \qquad (2)$$

where t_0 is the time to reach maximum power (800 μs in our case), σ is the full width at half maximum that was chosen to be 0.45 ms in order to simulate a realistic laser pulse duration. The numerical method used to solve the bioheat equation is based on a second-order method of finite differences in two dimensions [16]. The boundary conditions are those for continuous flux, except for the air-epidermis interface, which was chosen to be an isolator because of the small value for thermal conductivity of air relative to that of tissue. The maximal time increments Δt were calculated from the Fourier numbers [16] Fo_x, Fo_z, which give the criterion for numerical stability, i.e., $\Delta t < \min\{Fo_x, Fo_z\}$, where $Fo_x = 0.25\ (\Delta x)^2\ \rho C/\eta$ and $Fo_z = 0.25\ (\Delta z)^2\ \rho C/\eta$, and Δx, Δz the grid size in *x* and *z* direction. The simulations of

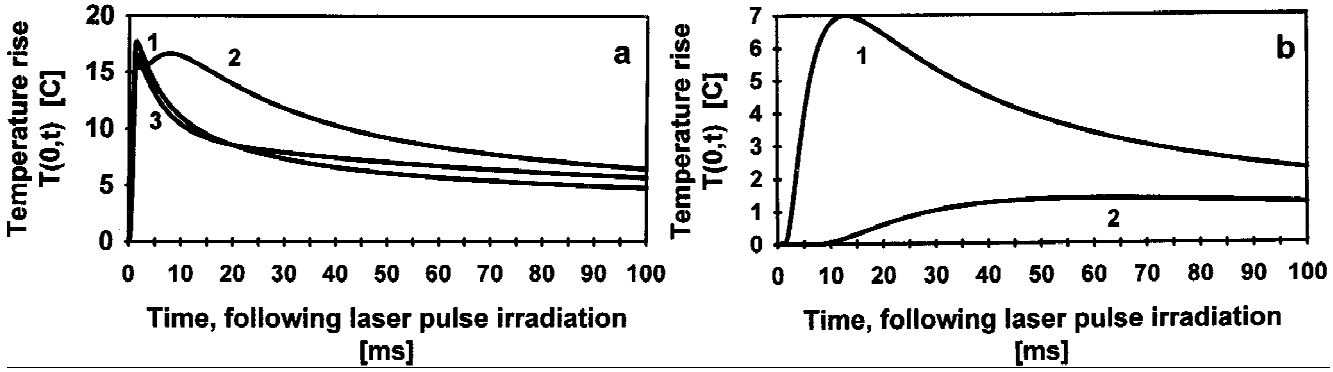

Fig. 2. (**a**) Skin surface temperature time course *T(0,t)* following laser pulse irradiation, at point (x = 0,z = 0), for "bloodless" skin (1) and for a 50 μm diameter blood vessel located at 100 μm (2) and at 200 μm (3) depth. (**b**) The net contribution of the blood vessel $T_B(0,t)$ to the skin surface temperature (curves 1 and 2).

heat flow were done in two dimensions. A one-dimensional calculation, although it is much faster, may differ from two-dimensional calculations, because of lateral heat flow effects. A typical two-dimensional run on a simulation time scale of 200 ms with time-step 50 μs takes 12 minutes.

Proposed Method

In the thermal linear region (no boiling or evaporation), the rise in temperature, *T(r,t),* is a linear superposition of thermal contributions from heat deposited into the blood vessels and into all other chromophores present in the skin volume. In order to distinguish between these two contributions, we proposed to use "bloodless" skin to simulate the contribution of all heat absorbing chromophores in the skin volume excluding the blood vessels. The set of optical parameters of dermis and epidermis for the bloodless skin was the same to that used for dermis and epidermis of the skin containing blood vessels (PWS skin) [11].

We propose to evaluate the net contribution of the blood vessels to the skin surface temperature rise by subtracting the temperature rise of "bloodless" skin from the temperature rise of PWS skin. However, the fluence rate distribution in the epidermis and dermis in "bloodless" skin is higher than the fluence rate distribution in a PWS skin. The reason is that in PWS skin part of the energy is absorbed by the blood vessels. Therefore, the temperature rise of "bloodless" skin has to be corrected to the same maximum temperature as the temperature rise in PWS skin. Subtracting this corrected temperature-time signal of "bloodless" skin from the signal of PWS skin results in a temperature-time curve that is closely related to the contribution of the blood vessels to the skin temperature rise.

Defining $T_B(r,t)$ as the net contribution of the blood vessels to $T(r,t)$ and $T_{BL}(r,t)$ the net contribution to $T(r,t)$ of "bloodless" skin, we have,

$$T_B(r,t) = T(r,t)—F_C(r)T_{BL}(r,t) \quad (3)$$

where the correction factor $F_C(r)$ is the ratio between the maximum temperature rise at the end of the laser pulse, $t = t_j$, in the normal PWS skin, $T(r,t_j)$ and "bloodless" skin $T_{BL}(r,t_j)$.

$$F_C(r) = T(r,t_j)/T_{BL}(r,t_j) \quad (4)$$

RESULTS

Figure 2a shows the skin surface temperature-time course following a diagnostic laser pulse for "bloodless" skin, $T_{BL}(0,t)$ (curve 1), and for a PWS involving a 50 μm diameter blood vessel located at 100 μm and at 200 μm depth, *T(0,t)* (curves 2 and 3, respectively). These curves are similar to the skin surface temperatures measured with a camera [8]. The blood vessel at 100 μm depth produces a second, delayed temperature peak, related to the blood vessel depth, but the blood vessel at 200 μm depth does not present any second temperature peak. Applying our method (Equations 3 and 4) on these curves gives the net contribution of the blood vessel to the skin surface temperature, $T_B(0,t)$, as shown in Figure 2b, curve 1 for 100 μm depth and curve 2 for 200 μm depth. These signals are induced only by the blood vessels and the time in which the maximum is achieved correlates only to blood vessel depth.

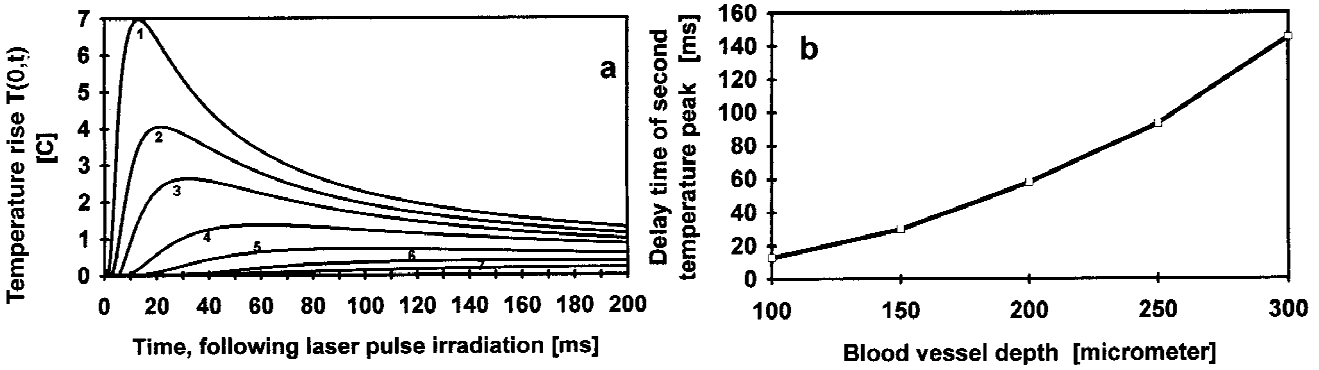

Fig. 3. (**a**) Corrected skin surface temperature—time course $T_B(r,t)$ (at x = z = 0) following a laser pulse induced by 50 μm diameter blood vessel located at different depths (100 μm (1), 125 μm (2), 150 μm (3), 200 μm (4), 250 μm (5), 300 μm (6), and 400 μm (7)). (**b**) Temperature peak delay time as a function of blood vessel depth, for a 50 μm diameter blood vessel.

Blood Vessel Depth

Figure 3a presents the net contribution $T_B(0,t)$ to the skin surface temperature, Equations (3) and (4), of a 50 μm diameter blood vessel located in different depths in the skin; 100 μm (curve 1), 125 μm (curve 2), 150 μm (curve 3), 200 μm (curve 4), 250 μm (curve 5), 300 μm (curve 6), and 400 μm (curve 7), following a 3J/cm^2 diagnostic laser pulse. The calculated correction factor was between 0.879 for 100 μm to 0.967 for 400 μm depth. Figure 3b shows the dependence of the time delay, in which the temperature $T_B(0,t)$ reaches its maximum, as a function of the blood vessel depth. Up to 300 μm depth, the temperature peak can be detected easily, for deeper blood vessels the net contribution signal $T_B(0,t)$ presents a plateau temperature peak.

Blood Vessel Diameter

The skin surface temperature due to blood vessels of different diameters, located at 150 μm depth, are presented in Figure 4a for 20μm (curve 1), 40μm (curve 2), 60μm (curve 3), 80μm (curve 4), and 100μm (curve 5) diameter. The time delay of the temperature peak is the same for all blood vessels, but the temperature peak amplitudes are higher for larger vessel diameters (see Fig. 4b showing a virtually perfect linear dependence). Figure 4 suggests that at a depth of 150 μm, a blood vessel of 10 μm diameter or larger can be assessed with our method. With increasing diameter at constant position of the axis of the blood vessel, the center of mass of the absorbed light in the blood shifts and the effective depth of the vessel appears shallower.

Melanin Content

The effect of the epidermal absorption coefficient (amount of melanin content) on the skin surface temperature is shown in Figure 5a. The temperature jump is higher for a higher absorption coefficient. The time needed to produce this jump does not show any absorption dependence. In all three cases the temperature jump is followed by a second delayed peak, but the time delay of this peak is different for each case, even though the blood vessel depth is the same. Figure 5b shows $T_B(0,t)$ for each case of melanin content. The delay time of the temperature peak is the same and shows no dependence on melanin content. The temperature peak correlates in an inverse way to the melanin content, higher temperature peak for lower melanin content. With increasing melanin content in the epidermis the temperature rise in the epidermis is higher. Less light reaches the blood vessel resulting in a lower temperature rise in the blood vessel and consequently a lower surface temperature rise.

Multiple Blood Vessels

Figure 6a presents $T_B(0,t)$ due to one blood vessel (curve 1) of 100 μm diameter at 110 μm skin depth and the temperature-time behaviour calculated at the same coordinate (0,0,0) caused by 16 blood vessels (curve 2), each of 100 μm diameter (arranged as sketched in Fig. 6b), occupying 10% of the PWS dermis volume. The time delay in which the temperature peak is achieved is the same (with 5% accuracy) in both cases. The contribution of the deeper vessels is observed only at longer times, by an increase in the cooling time

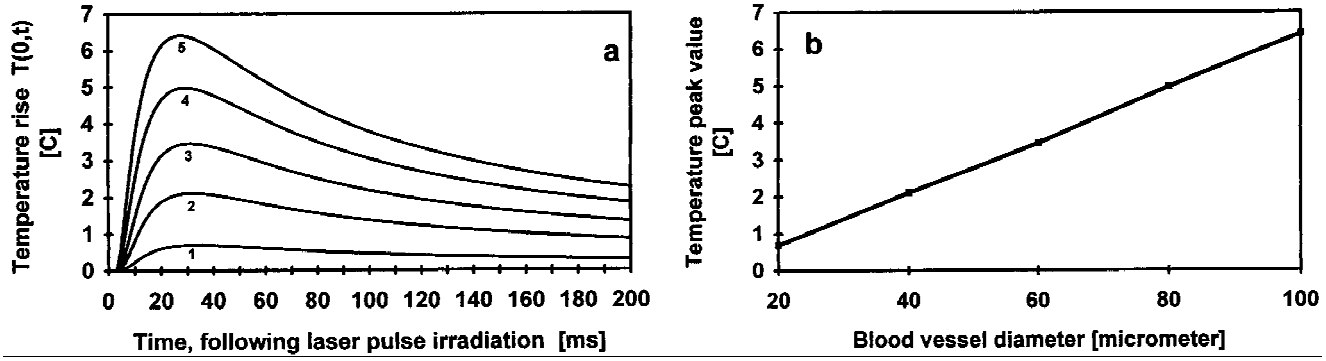

Fig. 4. (**a**) Corrected skin surface temperature—time course $T_B(r,t)$ (at x = z = 0) following a laser pulse induced by a blood vessel of different diameters (20 μm (1), 40 μm (2), 60 μm (3), 80 μm (4), and 100 μm (5)) located at 150 μm depth. (**b**) Temperature peak value as a function of blood vessel diameter at 150 μm depth.

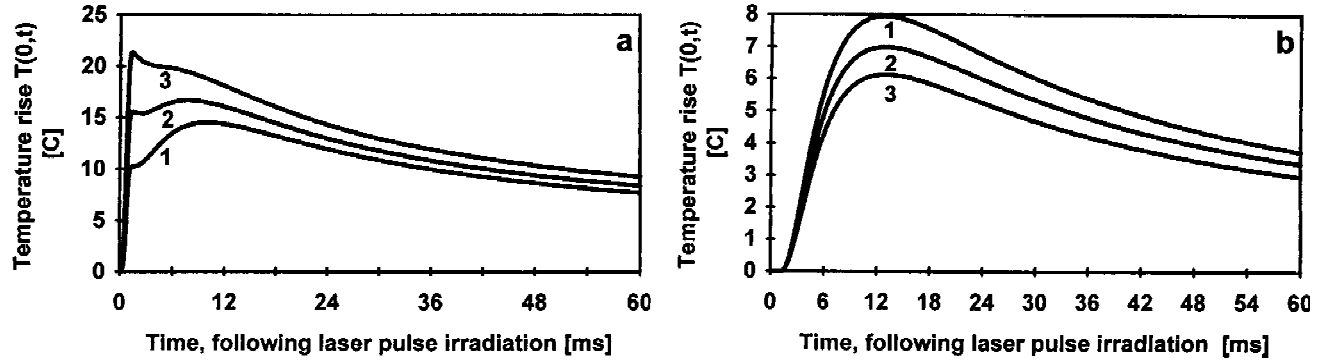

Fig. 5. (**a**) Skin surface temperature—time course $T(r,t)$ (at x = z = 0) following a laser pulse for a 50 μm diameter blood vessel located at 100 μm depth, for three epidermal absorption coefficients: 10.5 (1), 18.5 (2), and 28.5 (3) cm^{-1}. (**b**) The signal induced at the skin surface by a blood vessel, $T_B(0,t)$, of 50 μm diameter located at 100 μm depth for each epidermal absorption coefficient.

constant, compared to the case of one blood vessel. Figure 7 shows skin surface temperature-time courses at different locations relative to the upper central blood vessel of the blood vessel configuration of Figure 6b. The first location is exactly above the upper central blood vessel (x = 0, curve 1); the others are shifted in *x* direction by 100 μm (curve 2), 200 μm (curve 3), 300 μm (curve 4), and 400 μm (curve 5). Curves 1 and 5 belong to surface spots located exactly above a blood vessel and therefore present the same time dependence. Curves 2 and 4 refer to surface spots shifted 100 μm (horizontally) relative to a blood vessel and therefore present almost the same time dependence. Curve 3 presents a surface spot located between two blood vessels.

DISCUSSION

Single Blood Vessel Parameters

The skin surface temperature-time curves shown in Figure 2a are very similar to those measured by Jacques et al. [8] in PWS and in normal skin. The second delayed peak is interpreted [7,8] as the diffusion time of the heat deposited into the blood vessel to reach the skin surface, and therefore the delay time depends on the blood vessel depth. Of course, there is some correlation between such a delayed peak to the depth of the blood vessel, but the question is whether it is exactly equal to the diffusion time. Also, is the lack of a delayed peak an indication that there is no blood vessel present? The answer is no for both questions. The existence of a delayed peak depends on the competition between the temperature-time behaviour contributed by the epidermis, which is decreasing with time after the immediate jump, and the one contributed by the blood vessel, which is initially increasing with time followed by the decrease with time. If the absolute value of the latter is greater than that of the former, within a certain time region, a peak will be observable. The delay time in which such a peak may occur depends not only on the blood

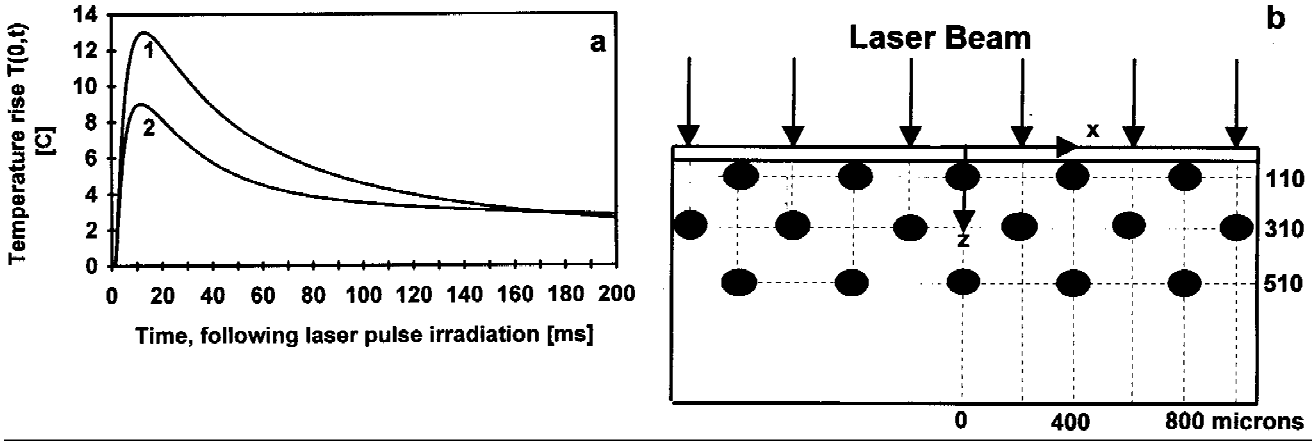

Fig. 6. Skin surface temperature time—course $T_B(r,t)$, Equations (3) and (4), at x = z = 0, following a laser pulse, (**a**) from one blood vessel of 100 μm diameter located at 110 μm (1) and from 16 blood vessels arranged in layers according to (**b**). The 16 blood vessels occupy 10% of the tissue dermal volume (b).

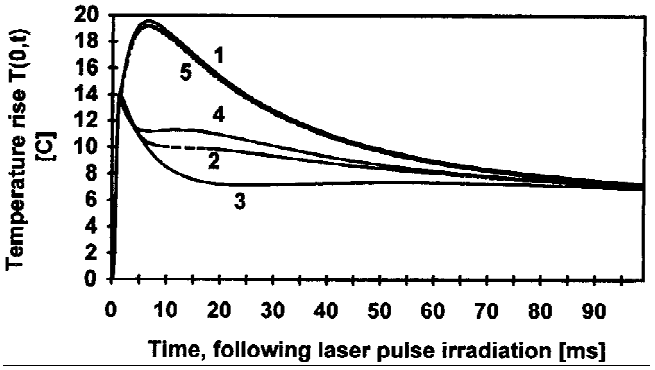

Fig. 7. Skin surface temperature-time course, $T(r,t)$, following a laser pulse from 16 blood vessels arranged as in Figure 6b for the central point, x = z = 0, (1), and for a shift in the x direction by 100 μm (2), 200 μm (3), 300 μm (4), and 400 μm (5).

vessel depth but also on the deposited energies into the epidermis and the blood vessel. Figure 5a clearly supports this argument. The time delay where the second peak occurs decreases as the energy deposited in the epidermis increases (larger melanin concentration). As a result, therefore, the skin surface temperature alone cannot offer the precise information required as to the depth of a blood vessel.

Using "bloodless" skin as a reference, it is possible to distinguish between the temperature-time signal induced by the blood vessels and by all the other absorbers, allowing assessment of the net contribution of the blood vessel to the skin surface temperature. The characteristic features of the blood vessel contribution, such as the time behaviour and the temperature peak amplitude, are correlated to blood vessel depth and diameter, respectively. The typical depth dependence is presented in Figure 3, for a fixed vessel diameter, where for deeper blood vessels the temperature peak is produced at longer time delays. The diameter dependence, presented in Figure 4 for a fixed depth, shows larger diameters induce higher temperature peaks. From a practical point of view, for 50 μm diameter blood vessel, our method seems to be applicable only for blood vessels located down to 300–400 μm depth, larger blood vessels can be detected even in deeper location. The reason is that at deeper vessel locations the temperature value of the signal induced by small diameter blood vessel is too small to be measured precisely by a thermocamera. Figure 2b compares, for the same blood vessel, skin surface temperature time-courses for scattering and absorbing skin (curve 1).

The depth dependence of the temperature peak time delay presented in Figure 3b has the form:

$$z = a\, t^{1/2} \tag{5}$$

where $a = (8.4 \pm 0.4)\ 10^{-2}$ [cm $s^{-1/2}$], measuring z in centimeters and t in seconds. This correlation formula is similar to that described by Jacques et al. [8], although their coefficient is smaller (0.0466). The linear dependence of the temperature peak on the blood vessel diameter seen in Figure 4b is an indication that the absorption

area of the blood vessels cross section, as a function of diameter, increases only in one dimension, perpendicular to the laser beam axis. This is caused by the limited penetration of the 577 nm in blood, and as a result the center of absorbing mass for large vessels is actually above the blood vessel center. For more accurate blood vessel diameter diagnosis, a longer wavelength 585 nm (or even 590 nm) may be used.

The immediate temperature jump contains information related to the degree of melanin content in the epidermis, higher temperature jump for higher melanin content. When this temperature value and its delay time are known, one can deduce the dermis-epidermis junction temperature and put a limit on the permitted laser energy for safe treatment without scarring.

Port Wine Stains Parameters

The "bloodless" skin model is successfully used, for one blood vessel case, to pick up the heat diffusion signal induced on the skin surface by a buried blood vessel. Can we use the same technique to pick up such a signal in real PWS lesions, where many blood vessels arranged in nonsymmetric configurations are involved? The results presented in Figure 6a, where the temperature peak was achieved at the same time delay for one blood vessel as for 16 blood vessels arranged to simulate a 10% blood volume PWS, means that this technique can be used to pick up the depth of the uppermost blood vessels only, but, in practice, these vessels are the target at any treatment session.

A major aspect of our technique is the use of "bloodless" skin, which represents the contribution of all the other absorbers excluding the blood vessels. The normal skin adjacent to the PWS lesion can, e.g., be used as a reference to present the contribution of all the absorbers excluding the PWS blood vessels. The argument for this is based on the assumption that the epidermis structure and melanin content of PWS skin and normal adjacent skin are identical.

The last aspect that should be discussed when using this technique in reality is the measured spot at the skin surface. In our model we can arbitrarily put the blood vessel to coincide with the laser beam axis and calculate the skin surface temperature of the spot located exactly above the blood vessel. But in reality, how can we locate the measured spot to be above a blood vessel when the blood vessel location is unknown? The results shown in Figure 7 present a differentiation (after 5–10 ms delay) in skin surface temperatures at different locations along the x axis, implying that the deduced PWS parameters may be in error when the location of the measurement is not exactly above a blood vessel. However, instead of measuring in one location, we can scan a line in any arbitrary direction that is incorporated in the laser beam spotsize. The highest temperature value along that line scan, at a certain time after the temperature jump, corresponds to a position above a blood vessel and that location should be chosen to record the temperature-time course. This procedure should be done twice, once in the PWS lesion and again in the adjacent normal skin. The only request is that the laser beam diameter should be large (>5 mm) in order to minimize photon density variation along the lateral axis. When that spot is known, we can apply our technique and use the temperature-time course to deduce the PWS parameters.

CONCLUSIONS

By modelling the skin surface temperature-time course, we have shown that the "bloodless" skin model provides a way to pick up the heat diffusion signal induced, on the skin surface, by subcutaneous blood vessels following a diagnostic laser pulse. Knowing this signal allows assessment of blood vessel depths, blood vessel diameters as well as the epidermal melanin content. We proposed that our technique can be applied to measure these parameters in real PWS lesions to provide a better insight of how to set the laser parameters in order to achieve better clinical results.

ACKNOWLEDGMENTS

This work was funded by the Dutch Organization for Scientific Research (NWO).

REFERENCES

1. Barsky SH, Rosen S, Geer DE, Noe JM. The nature and evaluation of port wine stains: a computer-assisted study. J Invest Dermatol 1980; 74:154–157.
2. Niechajev IA, Clodius L. Histology of port-wine stain. Eur J Plast Surg 1990; 13:79–85.
3. Anderson RR, Parrish JA. Selective photothermolysis: Precise microsurgery by selective absorption of pulsed radiation. Science 1983; 220:524–527.
4. Tan OT, ed. "Management and Treatment of Benign Cutaneous Vascular Lesions." Philadelphia: Lea & Febiger, 1992.

5. Goldman MP, Fitzpatrick RE. Treatment of Cutaneous vascular lesions. In: Goldman MP, Fitzpatrick RE, eds. "Cutaneous Laser Surgery." St. Louis, Mosby, 1994, pp 19–105.
6. van Gemert MJC, Welch AJ, Pickering JW, Tan OT, Gijsbers GHM. Wavelengths for laser treatment of port wine stains and telangiectasia. Lasers Surg Med 1995; 16:147–155.
7. Long FH, Anderson RR, Deutsch TF. Pulsed photothermal radiometry for depth profiling of layered media. Appl Phys Lett 1987; 51(25):2076–2078.
8. Jacques SL, Nelson JS, Wright WH, Milner TE. Pulsed photothermal radiometry of port-wine-stain lesions. Appl Opt 1993; 32(13):2439–2446.
9. Milner TE, Goodman DM, Tanenbaum BS, Nelson JS. Depth profiling of laser heated chromophores in biological tissues using pulsed Photothermal Radiometry. J Opt Soc Am A (submitted).
10. Verkruysse W, Pickering JW, Beek JF, Keijzer M, van Gemert MJC. Modelling the effect of wavelength on the pulsed dye laser treatment of port wine stains. Appl Opt 1993; 32:393–398.
11. van Gemert MJC, Welch AJ, Amin A. Is there an optimal treatment for port wine stains? Lasers Surg Med 1986; 6:76–83.
12. Smithies DJ, Butler PH. Modelling the distribution of laser light in port-wine stains with the Monte Carlo method. Phys Med Biol 1995; 40:701–733.
13. Henyey LG, Greenstein JL. Diffuse radiation in the galaxy. Astrophysics J 1941; 93:70–83.
14. Keijzer M. Light transport for medical laser treatment, PhD thesis, Delft, The Netherlands. 1993.
15. Lucassen GW, Verkruysse W, Keijzer M, van Gemert MJC. Light distribution in a port wine stain model containing multiple cylindrical and curved blood vessels. Lasers Surg Med 1996 (in press).
16. Carslaw HS, Jagger JC. Numerical methods. In: "Conduction of Heat in Solids." Oxford, Clarendon, 1986, pp 466–478.